

## Supplementary Information

### **Molecular engineering of theranostic molecule that detects A $\beta$ plaques, inhibits Iowa and Dutch mutation A $\beta$ self-aggregation and promotes lysosomal biogenesis for Alzheimer's disease**

Ashok Iyaswamy<sup>‡,1,2,\*</sup>, Xueli Wang<sup>‡,3,7</sup>, Hailong Zhang<sup>3</sup>, Karthick Vasudevan<sup>4</sup>,  
Dapkupar Wankar<sup>5</sup>, Kejia Lu<sup>1</sup>, Senthilkumar Krishnamoorthi<sup>1</sup>, Xin-Jie Guan<sup>1</sup>, Cheng-  
Fu Su<sup>1</sup>, Jia Liu<sup>1</sup>, Yuxuan Kan<sup>1</sup>, Ravindran Jaganathan<sup>6</sup>, Zhiqiang Deng<sup>1</sup>, Hung-Wing  
Li<sup>7,\*</sup>, Man Shing Wong<sup>3,\*</sup>, Min Li<sup>1,\*</sup>

<sup>1</sup>Mr. & Mrs. Ko Chi-Ming Centre for Parkinson's Disease Research, School of Chinese Medicine, Hong Kong Baptist University, Hong Kong SAR, China.

<sup>2</sup>Department of Biochemistry, Karpagam Academy of Higher Education, Coimbatore, India

<sup>3</sup>Department of Chemistry, Hong Kong Baptist University, Kowloon Tong, Hong Kong SAR, China.

<sup>4</sup>Department of Biotechnology, REVA University, Bangalore, India

<sup>5</sup>Faculty of Paramedical Sciences, Assam down town University, Guwahati, Assam, 781026, India

<sup>6</sup>Preclinical Department, Faculty of Medicine, Royal College of Medicine Perak, Universiti Kuala Lumpur, Perak, Malaysia

<sup>7</sup>Department of Chemistry, Chinese University of Hong Kong, Shatin, Hong Kong SAR, China.

<sup>8</sup>Present address: College of Pharmaceutical Sciences, Hebei University, Baoding 071002, China

\*Corresponding author:

Prof. Min Li (E-mail: [limin@hkbu.edu.hk](mailto:limin@hkbu.edu.hk)), School of Chinese Medicine, Hong Kong Baptist University, Kowloon Tong, Hong Kong. Tel: + 852-3411 2919, Fax: + 852-3411 2461.

\*Co-corresponding authors:

Dr. Ashok Iyaswamy (E-mail: [ashokenviro@gmail.com](mailto:ashokenviro@gmail.com), [iashok@hkbu.edu.hk](mailto:iashok@hkbu.edu.hk)) Dr. Hung-Wing Li ([hungwingli@cuhk.edu.hk](mailto:hungwingli@cuhk.edu.hk)) Prof. Man Shing Wong ([mswong@hkbu.edu.hk](mailto:mswong@hkbu.edu.hk))

<sup>‡</sup>Equally contributed to this work.

## Experimental:

### Synthesis of 9-(2-(2-methoxyethoxy)ethyl)-9H-carbazole 2.

To a solution of carbazole (3.34 g, 20 mmol) in DMF (80 mL) at 0 °C was added NaH (0.72 g, 30 mmol). After heating at 80 °C for 1.5 h, 1-chloro-2-(2-methoxyethoxy)ethane (3.31g, 24 mmol) was added dropwise. The resulting mixture was kept at 80 °C overnight. After cooling down to 0 °C, the reaction mixture was carefully quenched with water and extracted with ethyl acetate three times. The combined organic phase was washed with water and brine. Then the organic layer was dried over anhydrous sodium sulfate and the solvent was removed. The residue was purified by silica gel chromatography using petroleum ether and ethyl acetate as eluent (EA:PE = 1:3) to afford alkylated carbazole **2** (4.46 g) as brown oil in 83% yield.

<sup>1</sup>H NMR (400 MHz, CDCl<sub>3</sub>) δ 8.09 (d, *J* = 7.6 Hz, 2H), 7.46 (m, 4H), 7.23 (m, 2H), 4.51 (t, *J* = 6.4 Hz, 2H), 3.86 (t, *J* = 6.4 Hz, 2H), 3.52 (m, 2H), 3.42 (m, 2H), 3.31 (s, 3H). <sup>13</sup>C NMR (100 MHz, CDCl<sub>3</sub>) δ 140.5, 125.6, 122.8, 120.2, 118.9, 108.7, 71.8, 70.7, 69.1, 59.0, 43.0. MS (FAB) *m/z* Calcd for C<sub>17</sub>H<sub>19</sub>NO<sub>2</sub> 269.1 Found 269.2 [M]<sup>+</sup>.

**3-Bromo-9-(2-(2-methoxyethoxy)ethyl)-9H-carbazole 3.** To a solution of **2** (2 g, 7.4 mmol) in dichloromethane (60 mL) was added NBS (1.3 g, 7.4 mmol) portionwise in an ice-water bath. After complete addition, the solution mixture was warmed to room temperature and stirred overnight. The resulting solution was washed with water and brine. The organic phase was dried over anhydrous sodium sulfate and the solvent were then removed. The residue was purified by silica gel chromatography using ethyl acetate and petroleum ether (EA: PE = 1: 5) as eluent to afford **3** (1.75 g) in 68% yield as an oil that can turn into solid after standing.

<sup>1</sup>H NMR (400 MHz, CDCl<sub>3</sub>) δ 8.16 (d, *J* = 2.0 Hz, 1H), 8.01 (d, *J* = 8.0 Hz, 1H), 7.51 (dd, *J* = 8.0 Hz, 2.0 Hz, 1H), 7.44 (m, 2H), 7.34 (d, *J* = 8.4 Hz, 1H), 7.22 (m, 1H), 4.46 (t, *J* = 6.0 Hz, 2H), 3.83 (t, *J* = 6.0 Hz, 2H), 3.48 (m, 2H), 3.39 (m, 2H), 3.28 (s, 3H). <sup>13</sup>C NMR (100 MHz, CDCl<sub>3</sub>) δ 140.7, 139.2, 128.2, 126.3, 124.5, 122.8, 121.8, 120.4, 119.3, 111.7, 110.4, 109.0, 71.8, 70.7, 69.1, 59.0, 43.2. MS (FAB) *m/z* Calcd for C<sub>17</sub>H<sub>18</sub>BrNO<sub>2</sub> 347.0 Found 347.3 [M]<sup>+</sup>.

**Synthesis of 3-fluoro-9-(2-(2-methoxyethoxy)ethyl)-9H-carbazole 4.** To a solution

of 3-bromo-9-(2-(2-methoxyethoxy)ethyl)-9H-carbazole (3.23 g, 9.3 mmol) in dry THF (50 mL) was added *n*-BuLi (1.6 M, 8.7 mL, 13.9 mmol) at -78 °C. The resulting mixture was stirred for 50 min at -78 °C and then added with N-fluorobenzenesulfonimide (5.6 g, 18.6 mmol). The reaction mixture was allowed to warm to room temperature and stirred for 2 h before quenched with ammonia chloride solution. The organic layer was separated, dried over anhydrous sodium sulfate and evaporated under vacuum. The residue was purified by silica gel column chromatography eluting with 3:1 petroleum ether/ethyl acetate to give compound **4** in 65% yield.

<sup>1</sup>H NMR (400 MHz, CDCl<sub>3</sub>) δ 8.03 (d, *J* = 7.6 Hz, 1H), 7.73 (dd, *J* = 2.4 Hz, *J* = 8.8 Hz 1H), 7.50-7.44 (m, 2H), 7.39 (dd, *J* = 4.4 Hz, *J* = 8.8 Hz, 1H), 7.25-7.17 (m, 2H), 4.49 (t, *J* = 6.4 Hz, 2H), 3.86 (t, *J* = 6.4 Hz, 2H), 3.52-3.50 (m, 2H), 3.43-3.41 (m, 2H), 3.32 (s, 3H). <sup>13</sup>C NMR (100 MHz, CDCl<sub>3</sub>) δ 158.6, 156.2, 141.4, 137.1, 126.3, 123.4, 123.3, 122.6, 122.6, 120.6, 119.1, 113.6, 113.3, 109.7, 109.6, 109.2, 106.1, 105.9, 72.1, 71.0, 69.4, 59.2, 43.4. HRMS (MALDI-TOF) *m/z* Calcd for C<sub>17</sub>H<sub>18</sub>FNO<sub>2</sub> 287.1316, Found 287.1314[M]<sup>+</sup>.

**Synthesis of 3-bromo-6-fluoro-9-(2-(2-methoxyethoxy) ethyl)-9H-carbazole 5.** To a solution of compound 3-fluoro-9-(2-(2-methoxyethoxy)ethyl)-9H-carbazole (1.06 g, 3.71 mmol) in chloroform (20 mL) was added NBS (0.66 g, 3.71 mmol) batchwise in an ice-water bath. After complete addition, the reaction mixture was warmed to room temperature slowly and stirred overnight. The reaction mixture was washed with water and brine. The organic layer was dried over anhydrous sodium sulfate, filtrated and evaporated under reduced pressure to give compound **5** in 85% yield.

<sup>1</sup>H NMR (400 MHz, CDCl<sub>3</sub>) δ 8.09-8.06 (m, 1H), 7.63-7.60 (m, 1H), 7.52-7.50 (m, 1H), 7.36-7.26 (m, 2H), 7.21-7.16 (m, 1H), 4.40 (d, *J* = 5.6 Hz, 2H), 3.82-3.80 (m, 2H), 3.49-3.46 (m, 2H), 3.40-3.38 (m, 2H), 3.29 (s, 3H). <sup>13</sup>C NMR (100 MHz, CDCl<sub>3</sub>) δ 158.7, 156.3, 140.1, 137.4, 128.9, 124.2, 124.2, 123.2, 122.3, 122.2, 114.4, 114.1, 111.8, 110.8, 110.0, 109.9, 106.2, 106.0. HRMS (MALDI-TOF) *m/z* Calcd for C<sub>17</sub>H<sub>17</sub>BrFNO<sub>2</sub> 366.0499, Found 366.0502[M]<sup>+</sup>.

**Synthesis of 6-bromo-9-(2-(2-methoxyethoxy)ethyl)-9H-carbazole-3-carb-**

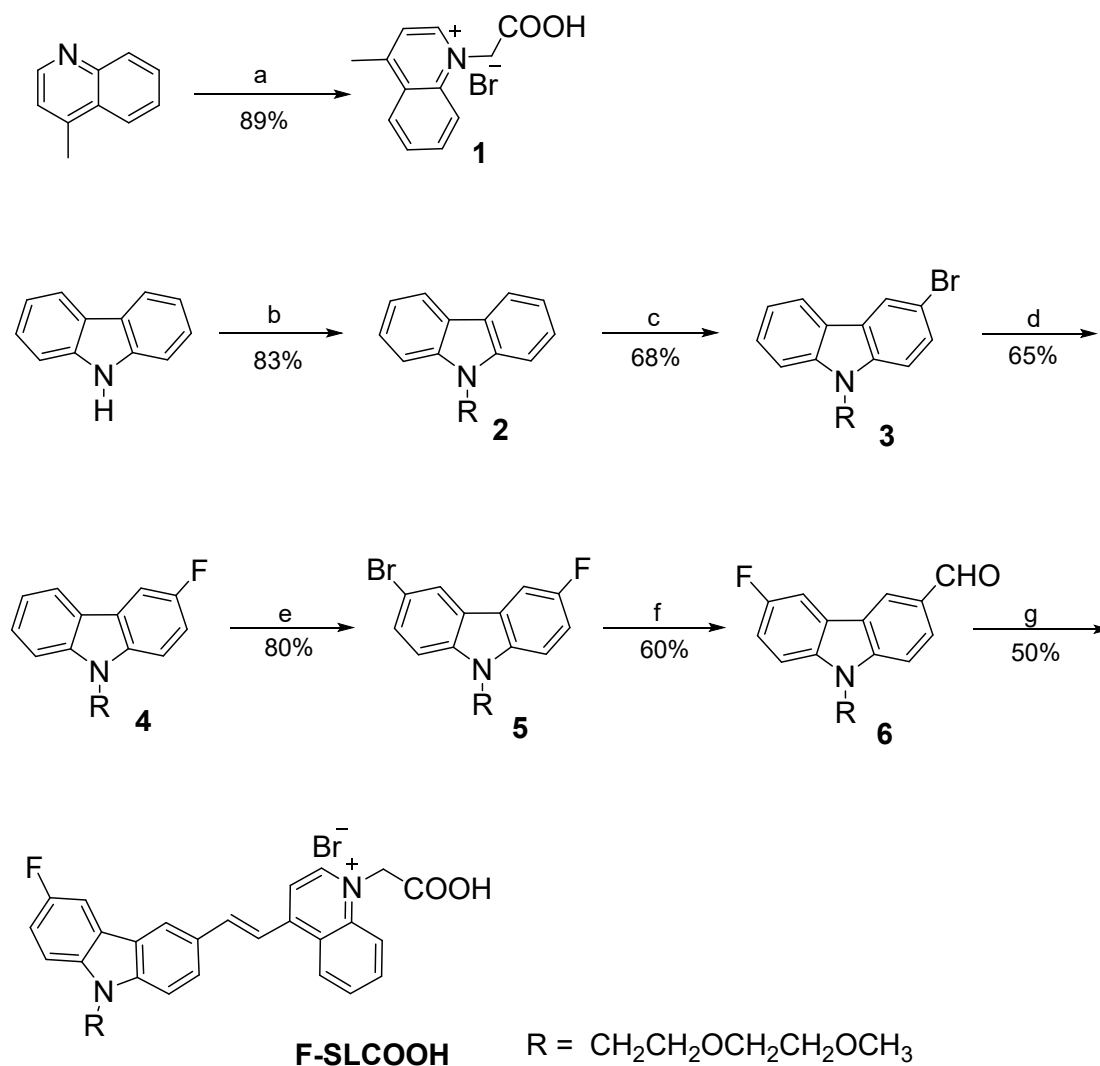
**aldehyde 6.** To a solution of 3-bromo-6-fluoro-9-(2-(2-methoxyethoxy)ethyl)-9H-carbazole (3.4 g, 9.3 mmol) in dry THF (50 mL) was added *n*-BuLi (1.6 M, 8.7 mL, 13.9 mmol) at -78 °C. The resulting mixture was stirred for 50 min at -78 °C and then added with N-formylmorpholine (1.86 mL, 18.6 mmol). The reaction mixture was allowed to warm to room temperature and stirred for 2 h before quenched with ammonia chloride solution. The organic layer was separated, dried over anhydrous sodium sulfate, filtrated and evaporated under vacuum. The residue was purified by silica gel column chromatography eluting with 2:1 petroleum ether/ethyl acetate to give compound **6** in 60% yield.

<sup>1</sup>H NMR (400 MHz, CDCl<sub>3</sub>) δ 10.08 (s, 1H), 8.53 (s, 1H), 8.02-8.00 (m, 1H), 7.80-7.77 (m, 1H), 7.54 (d, *J* = 8.8 Hz, 1H), 7.45 (dd, *J* = 4.0 Hz, *J* = 9.2 Hz 1H), 7.28-7.23 (m, 1H), 4.52 (t, *J* = 5.6 Hz, 2H), 3.88 (t, *J* = 5.6 Hz, 2H), 3.52-3.50 (m, 2H), 3.40 (d, *J* = 2.8 Hz, 2H), 3.28 (s, 3H). <sup>13</sup>C NMR (100 MHz, CDCl<sub>3</sub>) δ 191.8, 159.3, 156.9, 145.2, 137.8, 128.8, 127.5, 124.4, 123.7, 123.7, 123.7, 122.8, 114.8, 114.5, 110.6, 110.5, 109.8, 106.7, 106.4, 72.1, 71.0, 69.5, 59.2, 43.9. HRMS (MALDI-TOF) *m/z* Calcd for C<sub>18</sub>H<sub>18</sub>FNO<sub>3</sub> 316.1343, Found 316.1340 [M]<sup>+</sup>.

**(E)-1-(Carboxymethyl)-4-(2-(6-fluoro-9-(2-(2-methoxyethoxy)ethyl)-9H-carbazol-3-yl)vinyl)quinolinium bromide (F-SLCOOH).** A solution mixture of **1** (0.25 g, 0.8 mmol), **6** (0.25 g, 1.1 mmol) and piperidine (0.1 mL) in ethanol (40 mL) was heated to reflux overnight. After cooling down to room temperature, the organic solvent was removed. The residue was purified by precipitation from methanol and ethyl acetate to afford **F-SLCOOH** in 50% yield.

<sup>1</sup>H NMR (400 MHz, DMSO-*d*<sub>6</sub>) δ 9.15 (d, *J* = 6.4 Hz, 1H), 9.01 (d, *J* = 8.4 Hz, 1H), 8.86 (d, *J* = 36.8 Hz, 1H), 8.43 (d, *J* = 6.4 Hz, 1H), 8.30 (s, 1H), 818 (d, *J* = 16 Hz, 1H), 8.09 (d, *J* = 16 Hz, 1H), 8.08-7.98 (m, 1H), 8.01-7.91 (m, 1H), 7.86-7.64 (m, 2H), 7.50 (d, *J* = 7.9 Hz, 1H), 7.37 (t, *J* = 9.1 Hz, 1H), 7.13 (d, *J* = 7.7 Hz, 1H), 5.77 (s, 2H), 5.22 (t, *J* = 5.2 Hz, 2H), 4.61 (t, *J* = 5.2 Hz, 2H), 3.82-3.96 (m, 2H), 3.51-3.42 (m, 2H), 3.40 (s, 3H). <sup>13</sup>C NMR (100 MHz, DMSO-*d*<sub>6</sub>) δ 170.30, 156.08, 147.16, 145.01, 143.84, 143.14, 138.77, 137.70, 137.55, 137.14, 134.24, 132.36, 128.00, 125.52, 122.50, 121.87, 120.45, 119.63, 117.28, 115.12, 112.91, 110.61, 110.28,

69.82, 68.93, 59.72, 58.05, 54.86. HRMS (MALDI-TOF)  $m/z$  Calcd for  $C_{30}H_{29}FN_2O_4$   
[M]<sup>+</sup> 500.2105, Found 499.6591.



*Reagents and Condition:* a)  $BrCH_2COOH$ , EA, r.t.; b)  $ClCH_2CH_2OCH_2CH_2OCH_3$ , NaH, DMF, 80 °C;  
c) NBS, DCM, 0 °C to r.t.; d) *n*-BuLi, NFSI, THF, -78 °C to r.t.; e) NBS, DCM, 0 °C to r.t.; f) (1) *n*-  
BuLi, N-formylmorpholine, THF, -78 °C to r.t.; (2) **1**, piperidine,  $CH_3CN$ , reflux.

**Scheme S1.** Synthesis of F-SLCOOH.

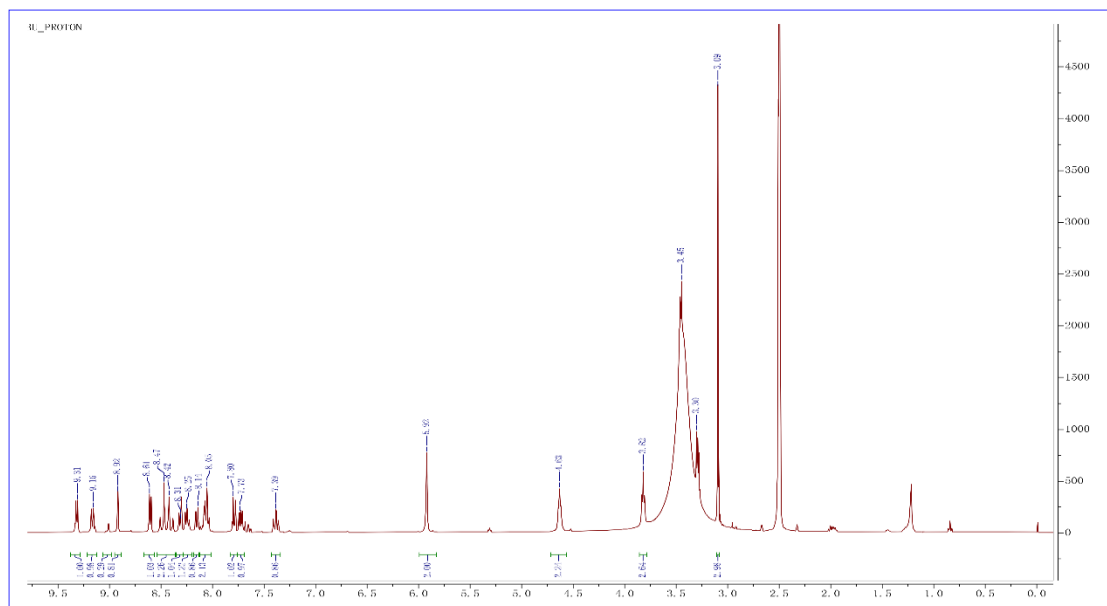


**Figure S1.**  $^1\text{H}$  NMR spectrum of F-SLCOOH

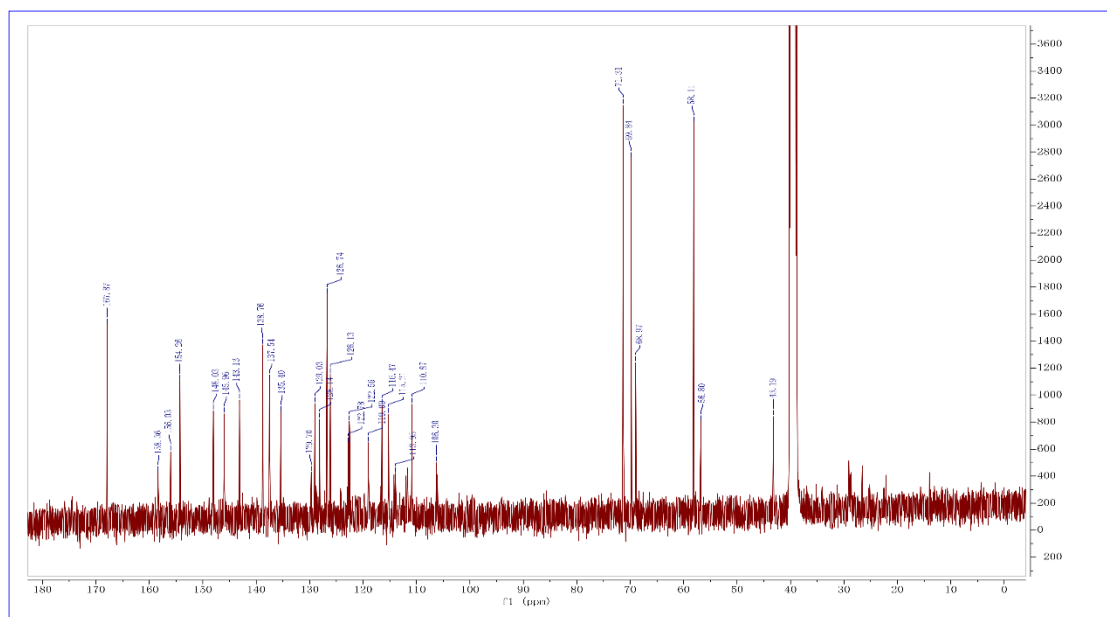


**Figure S2.**  $^{13}\text{C}$  NMR spectrum of F-SLCOOH.

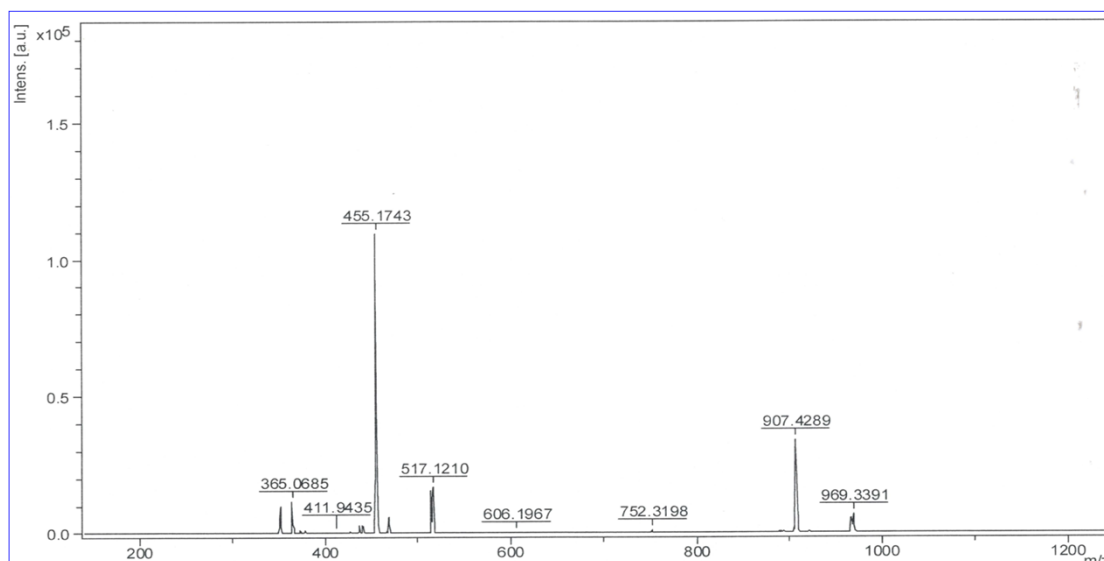
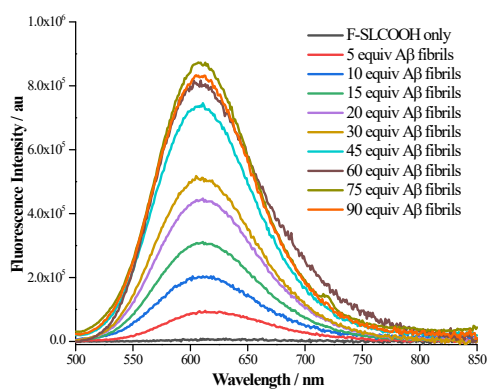
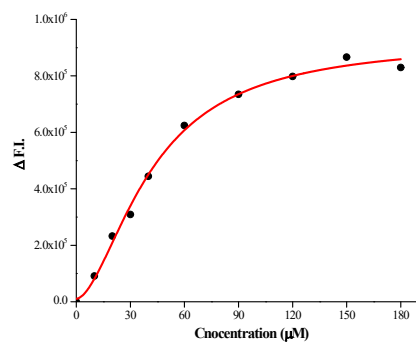


**Figure S3.** High-resolution mass spectrum of F-SLCOOH.

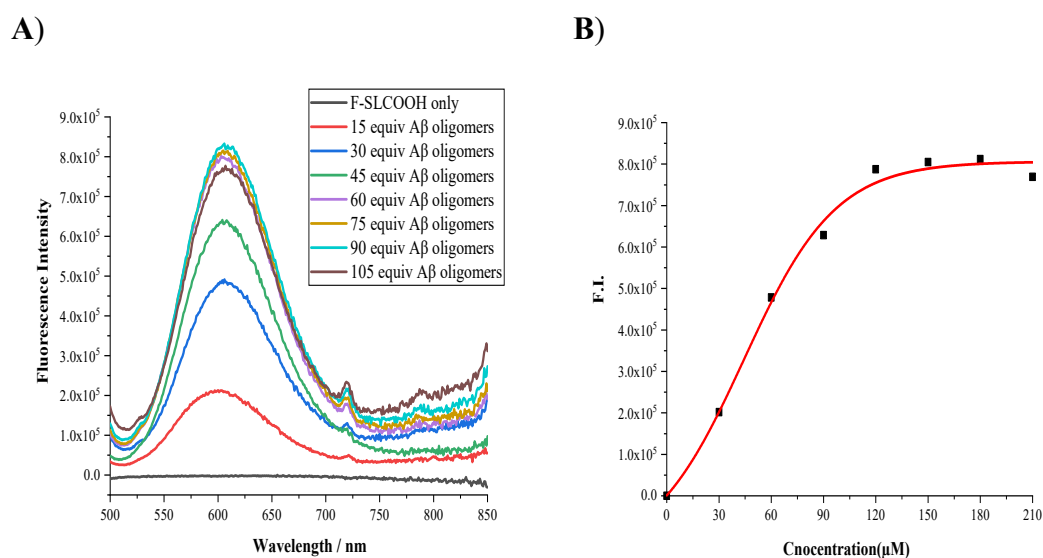
**A)**



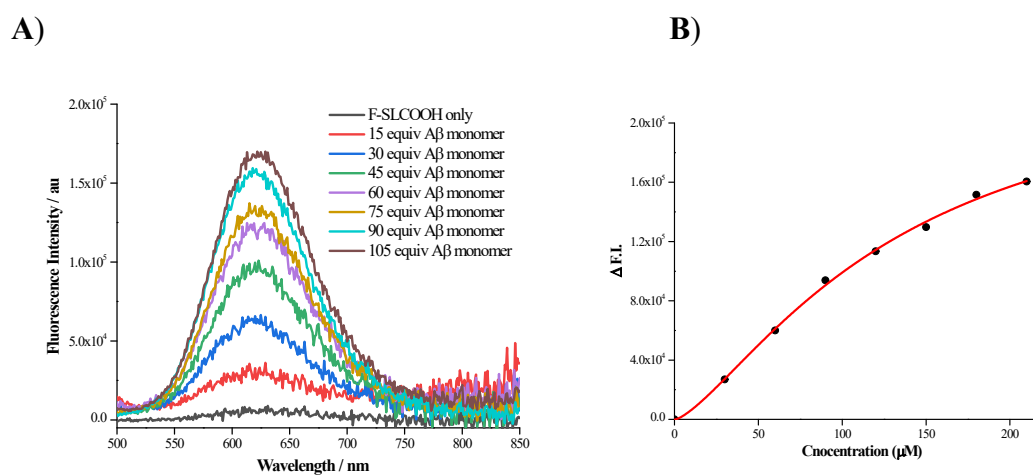
**B)**



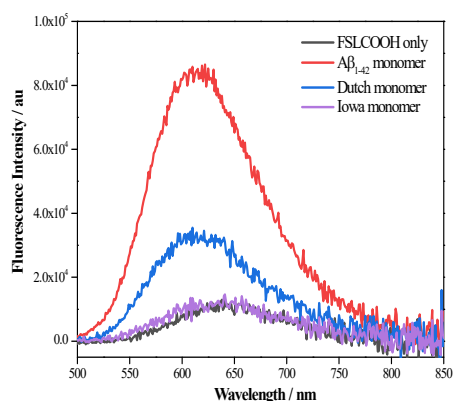
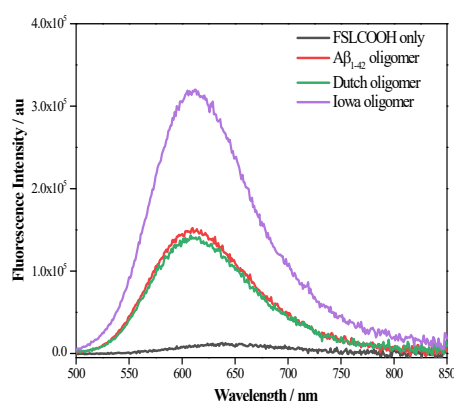
**Figure S4.** (A) Fluorescence spectra of F-SLCOOH (2  $\mu$ M) upon addition of various concentrations of A $\beta_{1-42}$  fibrils in 25 mM phosphate buffer (pH = 7.4). (B) The graph shows the curve fitting of the nonlinear analysis of intensity difference.



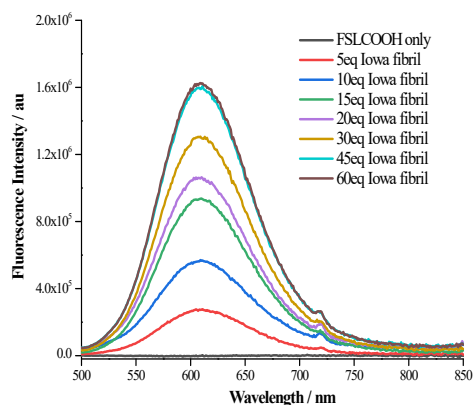
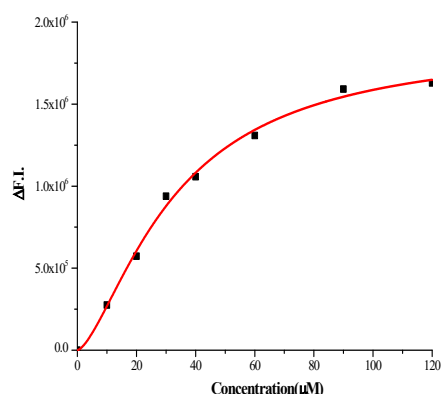
**Figure S5.** (A) Fluorescence spectra of F-SLCOOH (2 μM) upon addition of various concentrations of Aβ<sub>1-42</sub> oligomers in 25 mM phosphate buffer (pH = 7.4). (B) The graph shows the curve fitting of the nonlinear analysis of intensity difference.



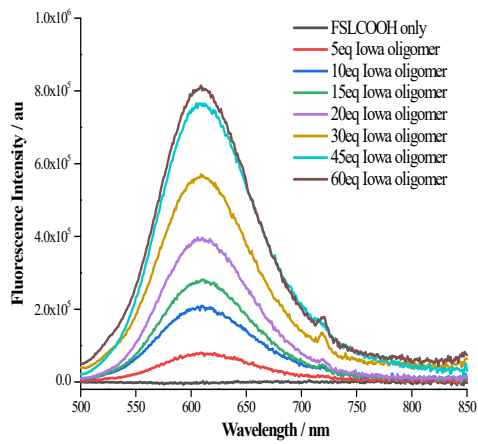
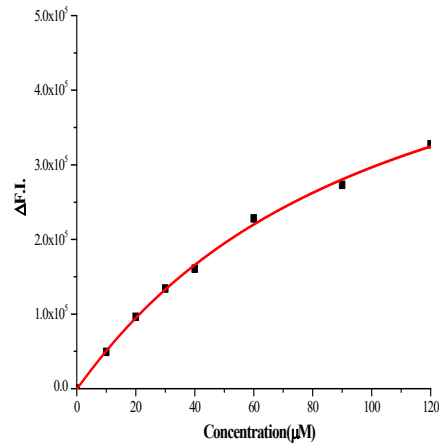
**Figure S6.** (A) Fluorescence spectra of F-SLCOOH (2 μM) upon addition of various concentrations of Aβ<sub>1-42</sub> monomers in 25 mM phosphate buffer (pH = 7.4). (B) The graph shows the curve fitting of the nonlinear analysis of intensity difference.

**A)****B)**

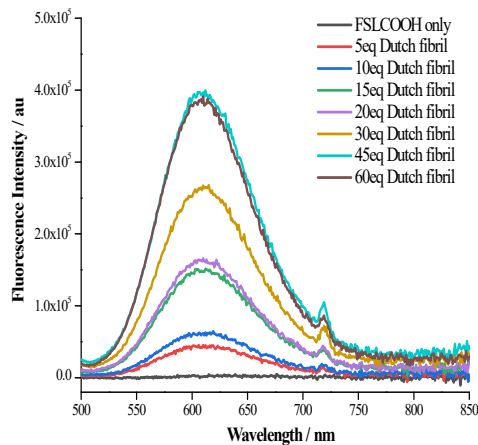
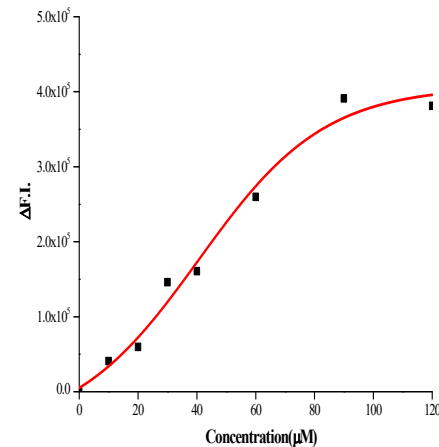
**Figure S7.** (A) Fluorescence spectra of F-SLCOOH (10 μM) in the presence of 10 μM Aβ<sub>1-42</sub> oligomers, E22Q Dutch Mutation oligomers, Iowa Mutation oligomers, measured in 25 mM phosphate buffer (pH = 7.4). (B) Fluorescence spectra of F-SLCOOH (10 μM) in the presence of 10 μM Aβ<sub>1-42</sub> monomers, E22Q Dutch Mutation monomers, Iowa Mutation monomers, measured in 25 mM phosphate buffer (pH = 7.4).

**A)****B)**

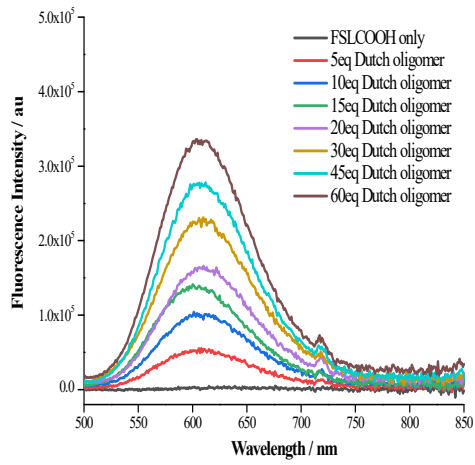
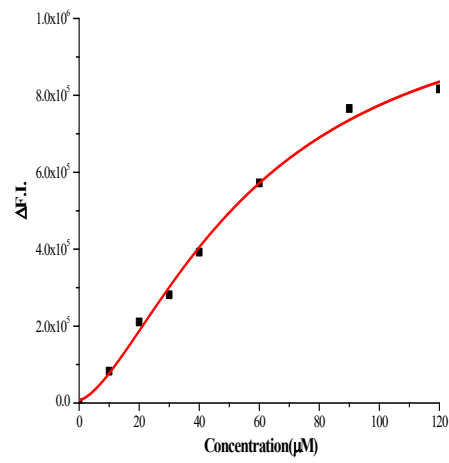
**Figure S8.** (A) Fluorescence spectra of F-SLCOOH (2 μM) upon addition of various concentrations of Iowa Mutation fibrils measured in 25 mM phosphate buffer (pH = 7.4). (B) The graph shows the curve fitting of the nonlinear analysis of intensity difference.

**A)****B)**

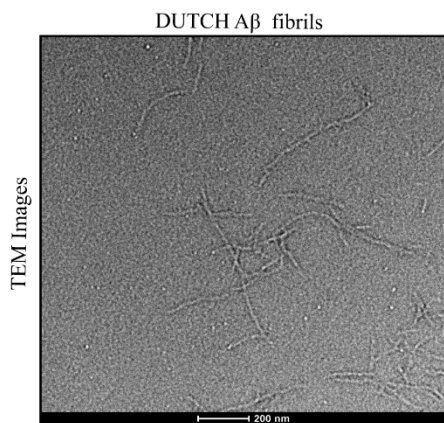
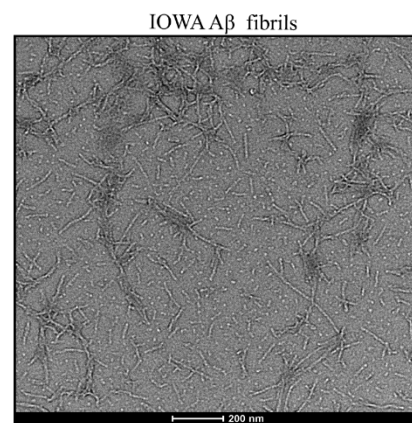
**Figure S9.** (A) Fluorescence spectra of F-SLCOOH (2  $\mu\text{M}$ ) upon addition of various concentrations of Iowa Mutation oligomers measured in 25 mM phosphate buffer (pH = 7.4). (B) The graph shows the curve fitting of the nonlinear analysis of intensity difference.

**A)****B)**

**Figure S10.** (A) Fluorescence spectra of F-SLCOOH (2  $\mu\text{M}$ ) upon addition of various concentrations of E22Q Dutch Mutation fibrils measured in 25 mM phosphate buffer (pH = 7.4). (B) The graph shows the curve fitting of the nonlinear analysis of intensity difference.

**A)****B)**

**Figure S11.** (A) Fluorescence spectra of F-SLCOOH (2  $\mu\text{M}$ ) upon addition of various concentrations of E22Q Dutch Mutation oligomers measured in 25 mM phosphate buffer (pH = 7.4). (B) The graph shows the curve fitting of the nonlinear analysis of intensity difference.

**A****B**

**Figure S12.** (A) Transmission electron microscopic images of E22Q Dutch Mutation A $\beta$  fibrils. (B) Transmission electron microscopic images of Iowa Mutation A $\beta$  fibrils.

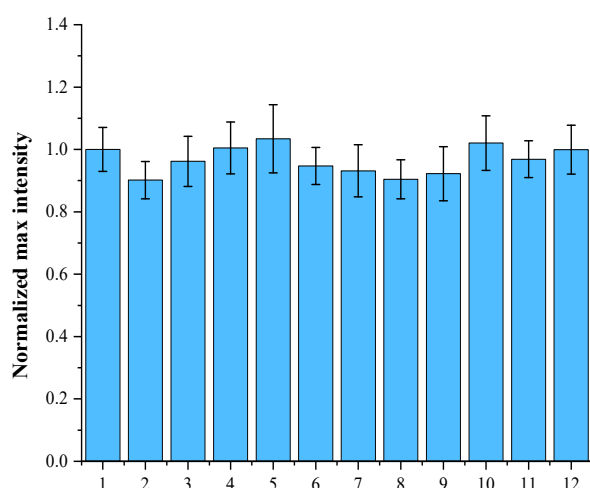


**Figure S13. (A)** The selectivity of F-SLCOOH (10  $\mu$ M) in response to various bioactive small molecules and metal ions (300  $\mu$ M) in PB after 2 h. 1 to 12 represent blank, Valine, Aspartic, Arginine, Phenylalanine,  $Mg^{2+}$ ,  $Ca^{2+}$ ,  $Hg^{2+}$ ,  $Cu^{2+}$ ,  $Ag^+$ ,  $K^+$ ,  $Zn^{2+}$ . Data are expressed as the mean  $\pm$  SD of three independent measurements (n=3).

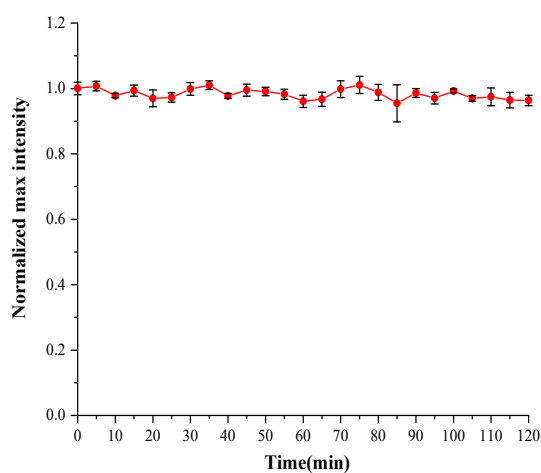


**Figure S14. (A)** Photostability of the F-SLCOOH (30  $\mu$ M) under ambient light illumination over a period of 120 min at ambient temperature in 25 mM phosphate buffer (pH = 7.4). All the spectra were obtained with the excitation wavelength of 480 nm and recorded the fluorescence intensity at the emission wavelength of 693 nm. Data are expressed as the mean  $\pm$  SD of three independent measurements (n = 3).

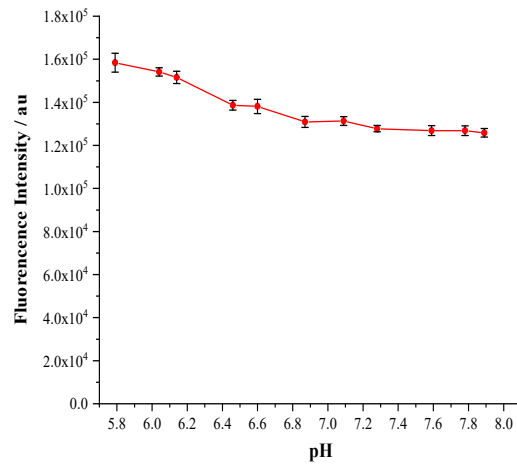
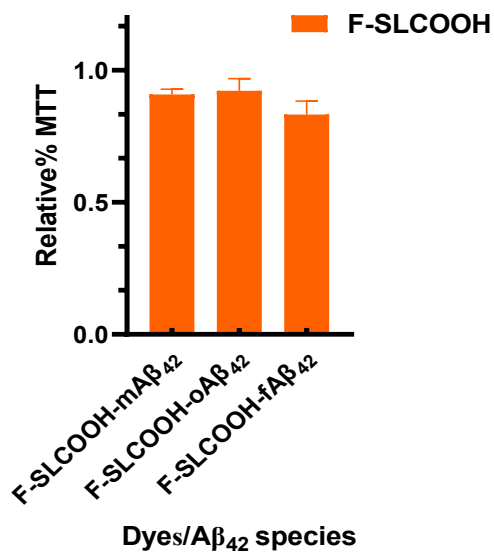


**Figure S15. (A)** The pH effect on the fluorescence intensity of F-SLCOOH (30  $\mu$ M) in 0.2 M phosphate buffer. Data are expressed as the mean  $\pm$  SD of three independent measurements (n = 3).

**A)**



**B)**

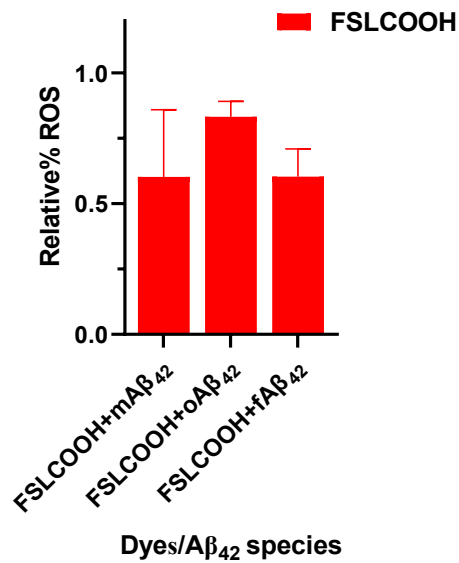


**Figure S16. (A)** The graph reveals the A $\beta_{1-42}$  monomer, oligomers and fibril-induced cytotoxicity in neuronal cells against the treatment with F-SLCOOH. **(B)** The graph reveals the reduction of ROS generation levels upon A $\beta_{1-42}$  monomer, oligomers and fibril treatment in neuronal cells against the treatment with F-SLCOOH. The relative cytotoxicity expressed in both MTT and ROS assays was calculated from the

cytotoxicity measured for different forms of A $\beta$  species with F-SLCOOH relative to that without it, i.e., (F-SLCOOH + A $\beta$  monomer) / monomer; (F-SLCOOH + oligomer) / oligomer; and (F-SLCOOH + fibril) / fibril. Three independent trials were analysed, and the results were expressed as mean  $\pm$  SEM.

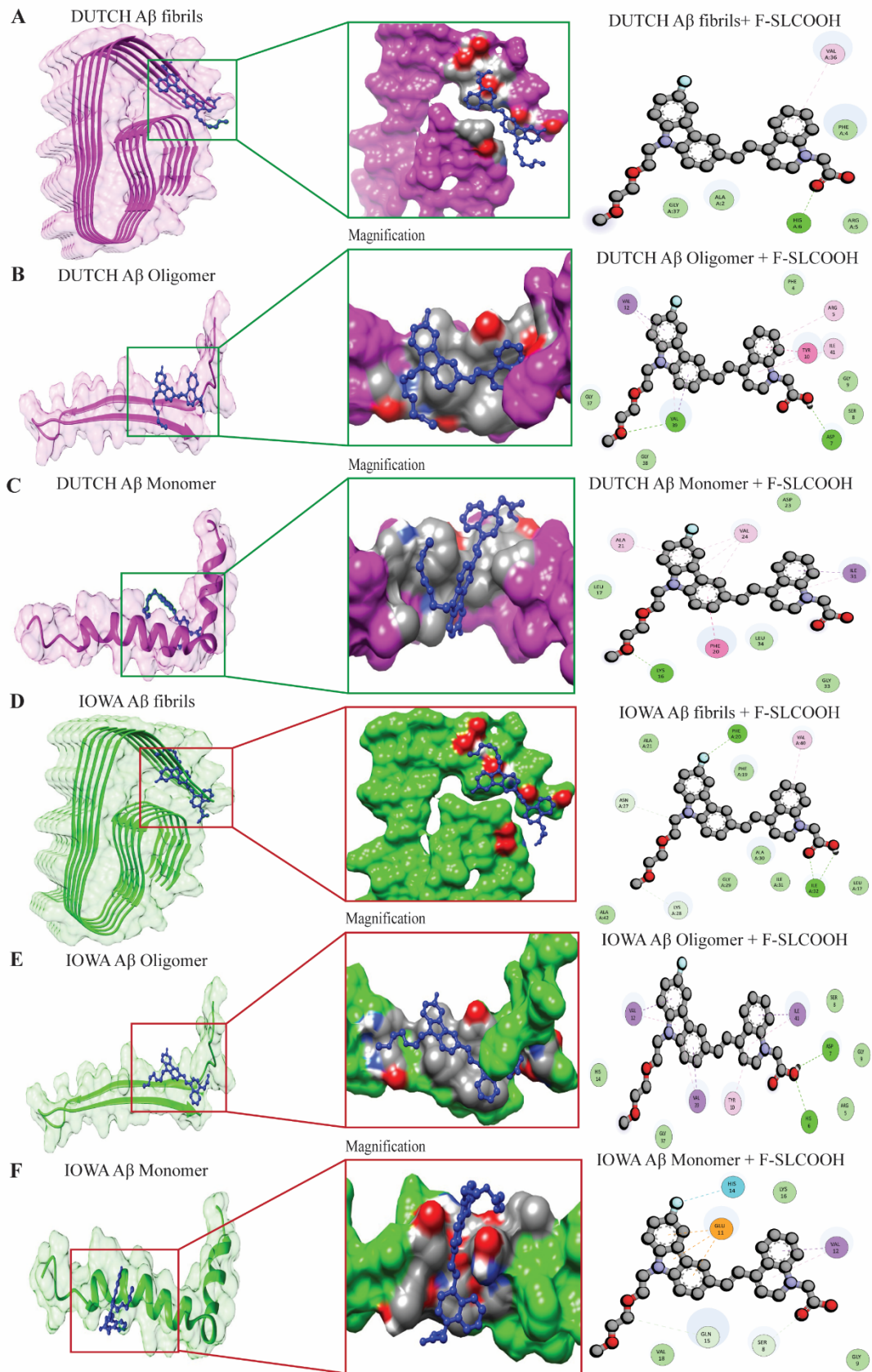


**Figure S17.** Binding pattern of F-SLCOOH with the ligand binding domain of DUTCH mutation A $\beta$  (A) fibril, (B) oligomer and (C) monomer. Binding pattern of

F-SLCOOH with the ligand binding domain of IOWA mutation A $\beta$  (**D**) fibril, (**E**) oligomer and (**F**) monomer.

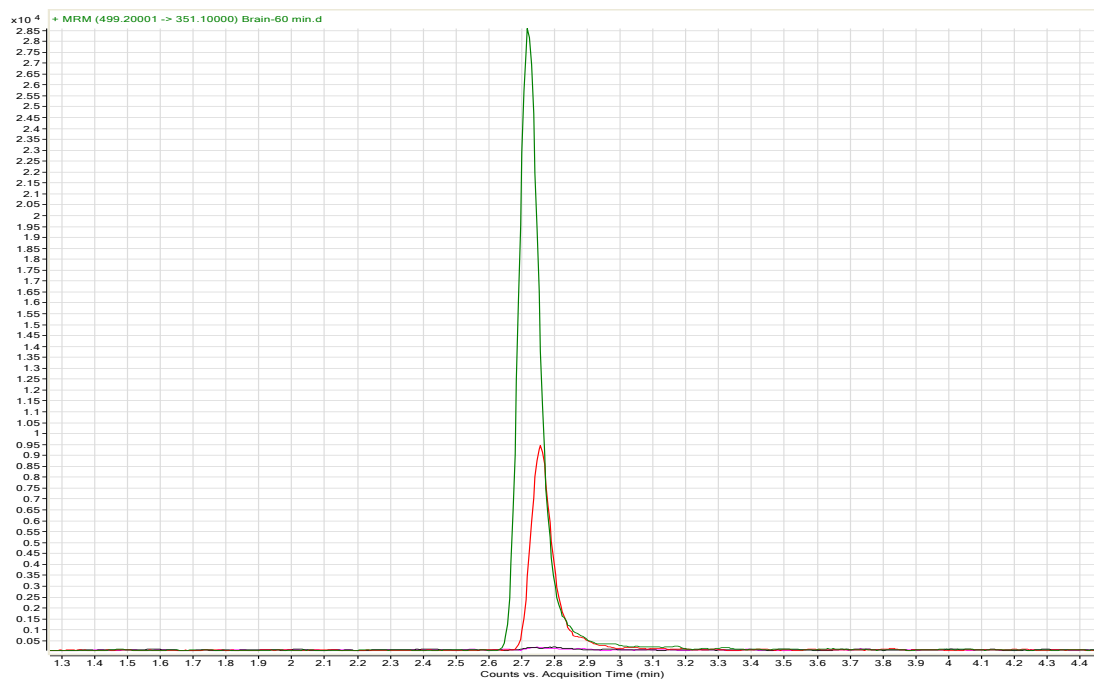
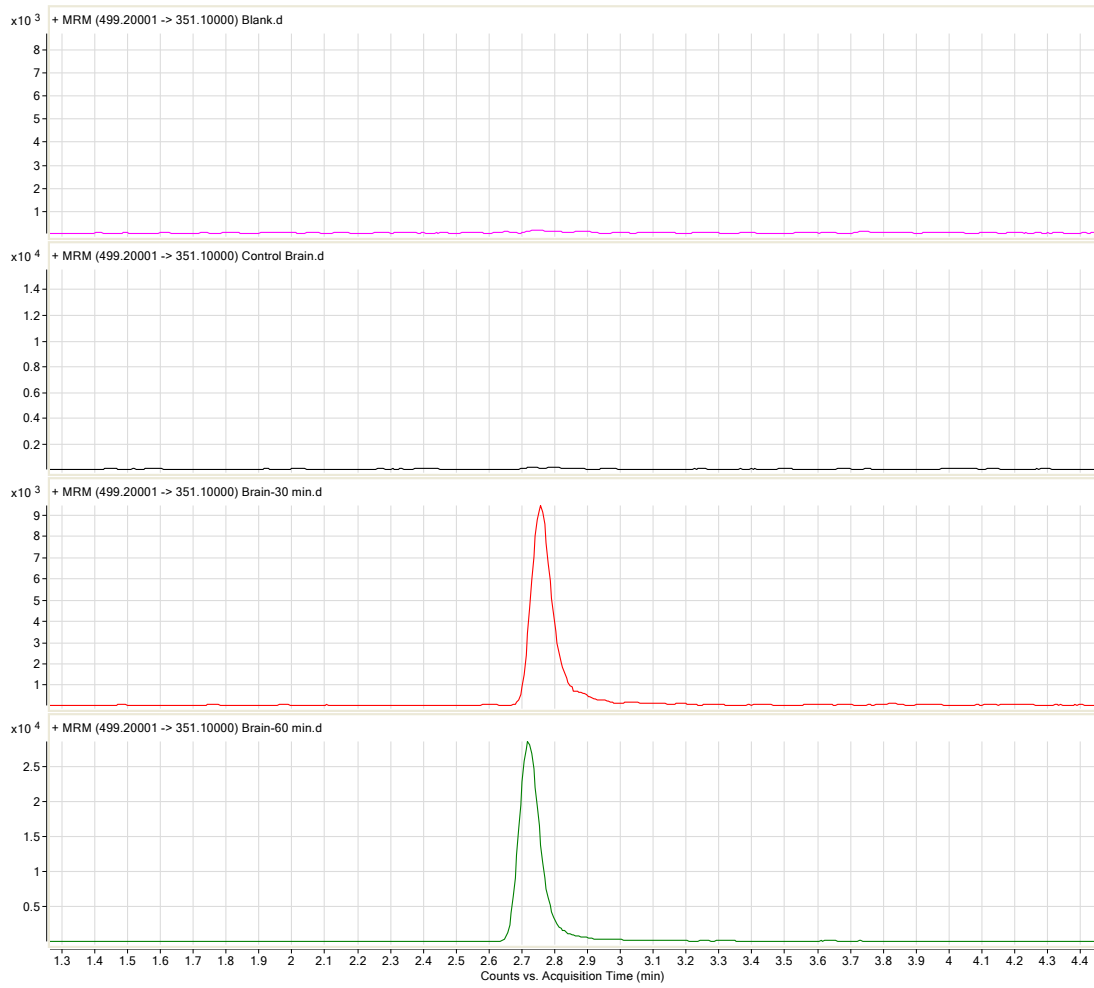


**Figure S18.** The bioavailability concentration of F-SLCOOH in the whole brain of WT animal (C57/BL6) at 0, 30 and 60 minutes after intraperitoneal administration of 10 mg/kg of F-SLCOOH.

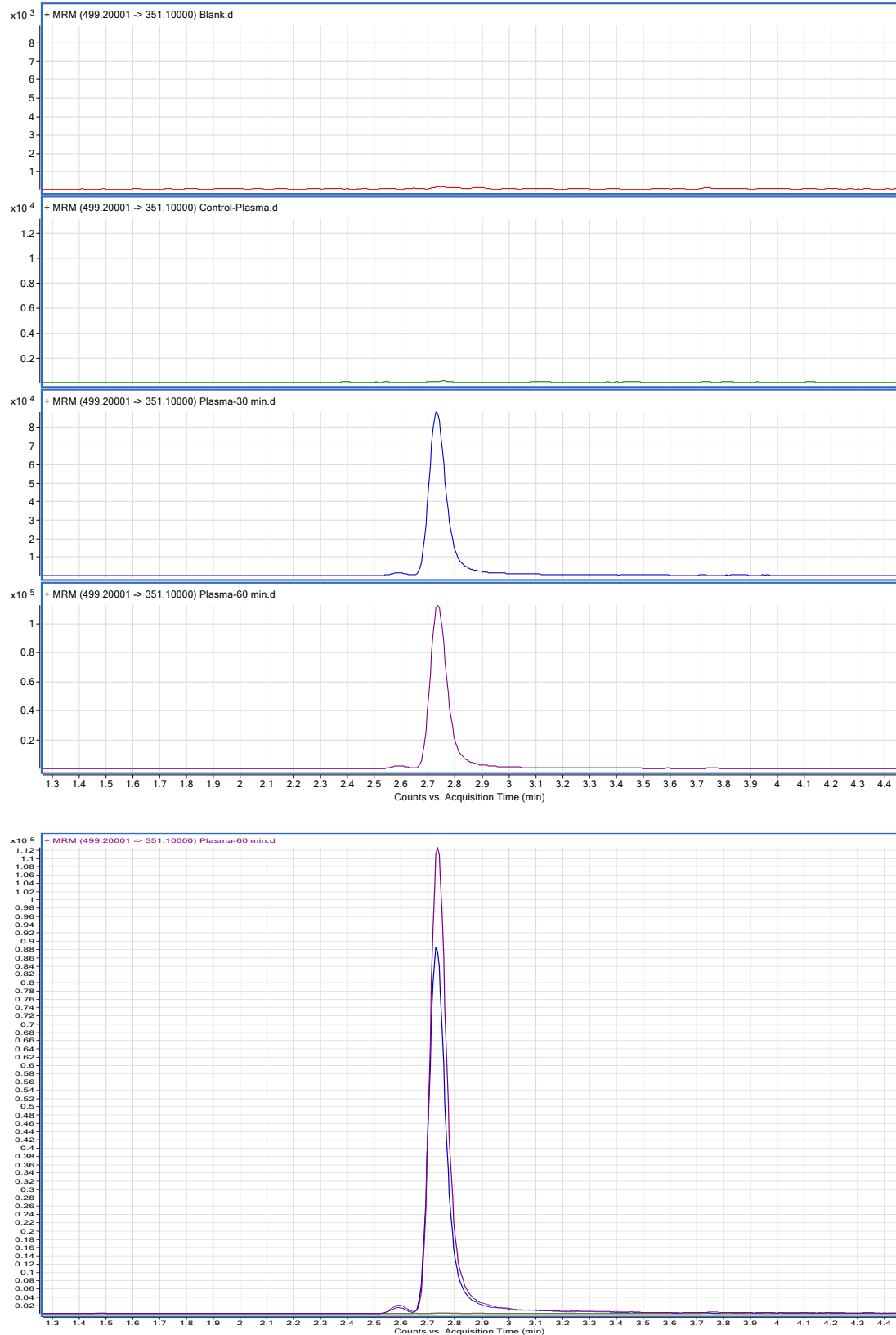


**Figure S19.** The bioavailability concentration of F-SLCOOH in the plasma of WT animal (C57/BL6) at 0, 30 and 60 minutes after intraperitoneal administration of 10 mg/kg of F-SLCOOH.

F-SLCOOH	A $\beta$ <sub>1-42</sub> monomer	A $\beta$ <sub>1-42</sub> oligomer	A $\beta$ <sub>1-42</sub> fibril	Tau*	$\alpha$ -Synuclein	BSA
Dissociation constant ( $K_d$ ) ( $\mu$ M)	131.54 $\pm$ 24.42	44.27 $\pm$ 7.92	41.80 $\pm$ 3.09	83.03 $\pm$ 284.89	60.78 $\pm$ 29.08	42.44 $\pm$ 8.95

\*Due to solubility problem, the use of high concentration was not possible which limited the data points used for curve fitting leading to a large error.

**Figure S20.** Comparison of dissociation constants ( $K_d$ ) of F-SLCOOH with various A $\beta$  species, tau,  $\alpha$ -Syn, and BSA as determined from the fluorescence titration of F-SLCOOH with various proteins.

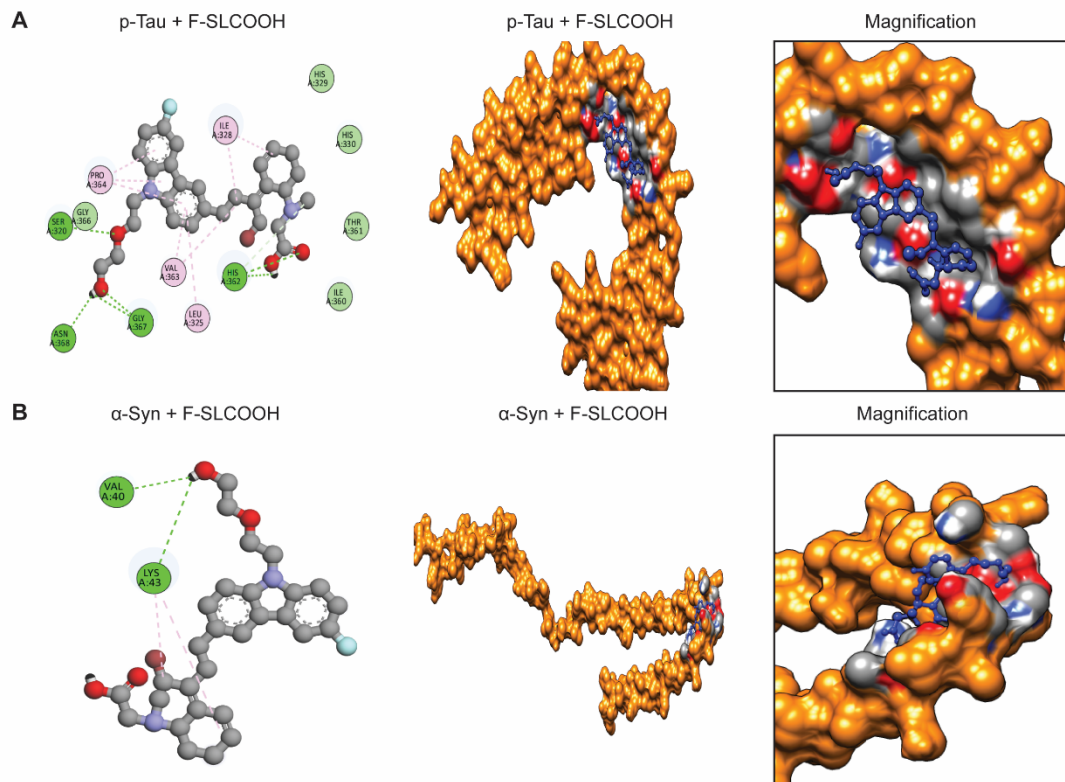


**Figure S21.** Binding motif of F-SLCOOH with the ligand binding domain of (A) p-Tau and (B)  $\alpha$ -Syn calculated by molecular docking. The docking binding affinity of p-Tau + F-SLCOOH was -6.0 kcal/mol and  $\alpha$ -Syn + F-SLCOOH was -5.5 kcal/mol.

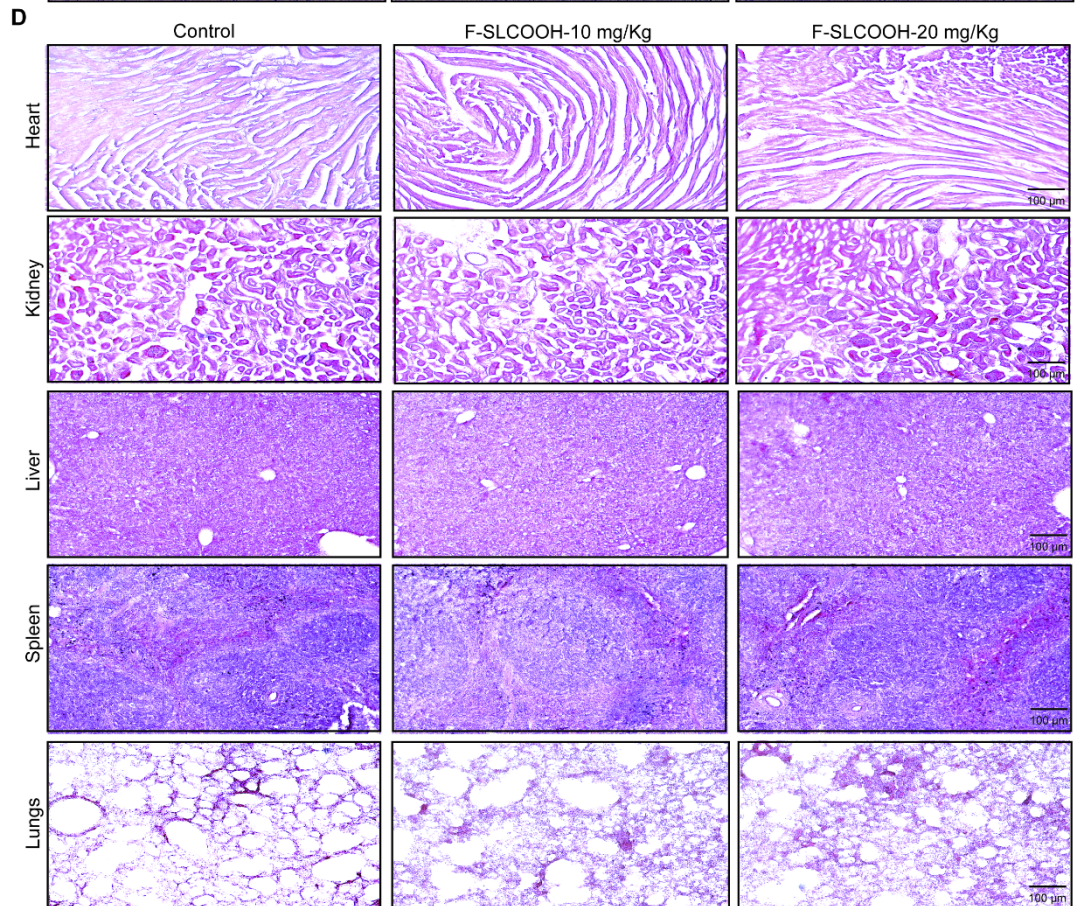
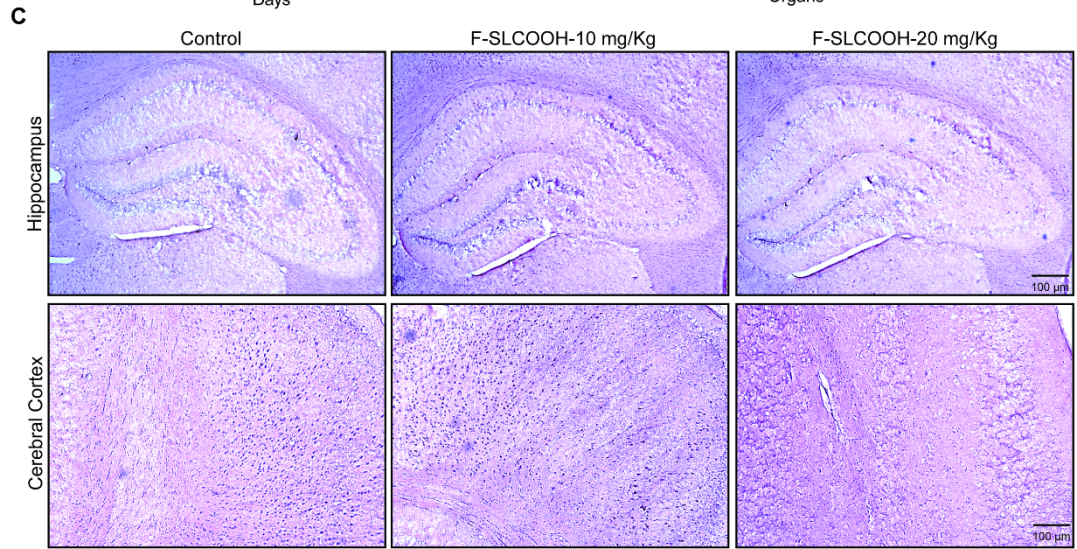
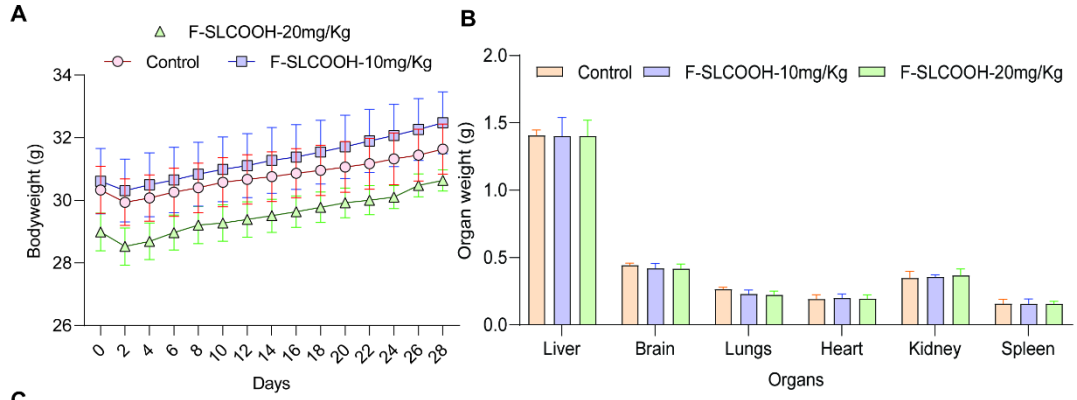


**Figure S22.** Acute toxicity of F-SLCOOH in WT (C57BL/6) mice. **(A)** F-SLCOOH did not cause any toxicity and interfere in the bodyweight change during the 28 days treatment period. **(B)** After 28 days of treatment, F-SLCOOH did not cause any toxicity or changes in organ weight of the treated WT animals. **(C-D)** The 28 days of F-SLCOOH treatment did not cause any histopathological changes in the brain regions and the other organs namely Liver, Heart, Spleen, Kidney, and Lungs in the treated WT animals. Bar diagram represents mean  $\pm$  SEM. (Treatment group compared with Control group, one-way ANOVA with Dunnett's multiple comparison test). For animal experiments each group has 6 animals, every group had N = 6, and compared among the number of animals.

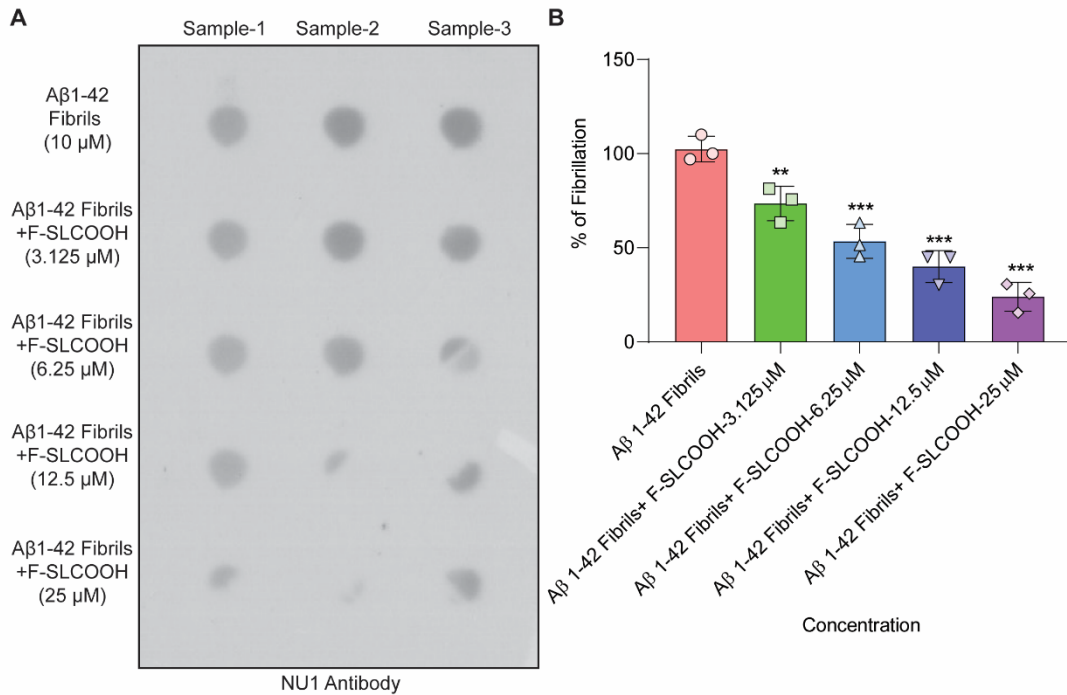


**Figure S23.** **(A)** F-SLCOOH dose dependently inhibited the fibril formation of Aβ in the anti-Aβ fibrillation assay using dot blot study. **(B)** The corresponding dose-dependent inhibition of the Aβ fibril formation given in bar graph. Each data point represents the average of three replicates and data represented as mean  $\pm$  SEM.

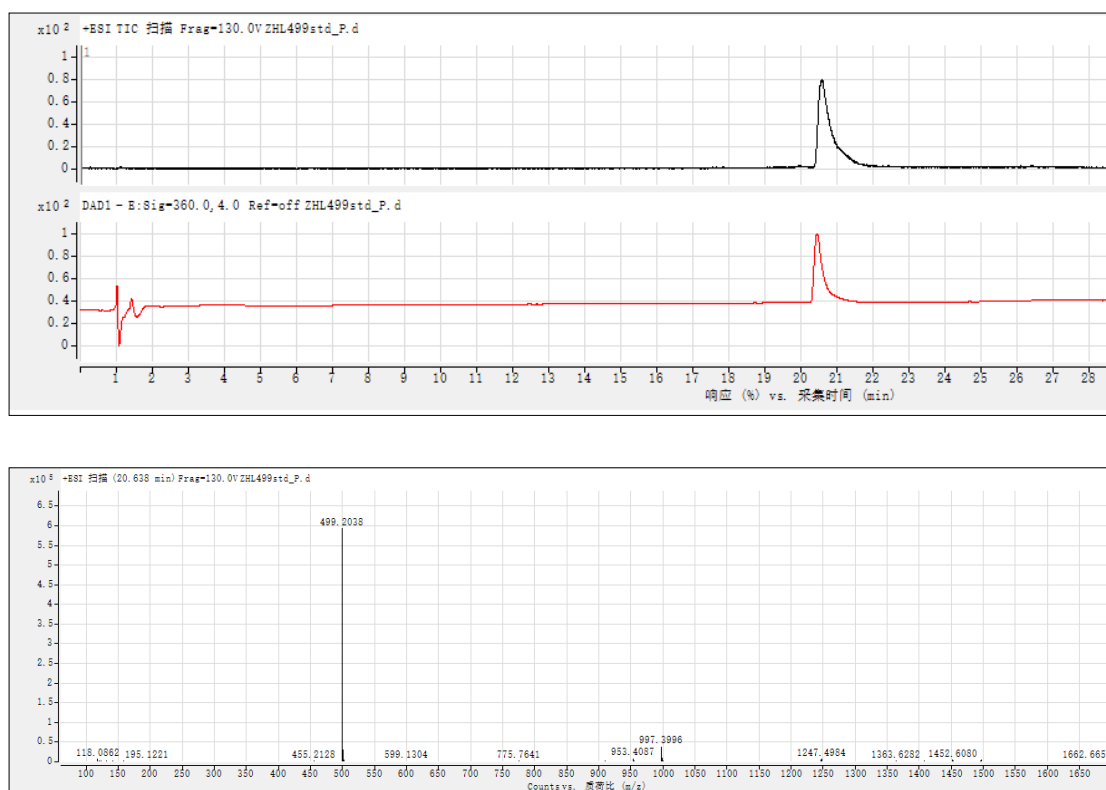


**Figure S24.** HPLC profile of F-SLCOOH analyzed using UHD Accurate-Mass Q-TOF LC/MS (Agilent Technologies).



**Figure S25. (A&B)** Bright field image of SH-SY5Y cells treated with F-SLCOOH (20 μM) with or without Aβ<sub>1-42</sub> (20 μM) fibrils, Iowa Aβ fibrils and Dutch Aβ fibrils for 24 hours.